Neurobiology of Pain 12 (2022) 100106

Contents lists available at ScienceDirect

Neurobiology of Pain

journal homepage: www.sciencedirect.com/journal/neurobiology-of-pain

Sex-distinct microglial activation and myeloid cell infiltration in the spinal cord after painful peripheral injury

Nolan A. Huck [a], Lauren J. Donovan [a], Huaishuang Shen [a,b], Claire E. Jordan [a], Gabriella P.B. Muwanga [a,c], Caldwell M. Bridges [a], Thomas E. Forman [a], Stephanie A. Cordonnier [a], Elena S. Haight [a], Fiona Dale-Huang [a], Yoshinori Takemura [a,d], Vivianne L. Tawfik [a,*]

[a] Department of Anesthesiology, Perioperative and Pain Medicine, Stanford University, Stanford, CA 94305, USA
[b] Department of Orthopedic Surgery, First Affiliated Hospital of Soochow University, Suzhou 215000, China
[c] Neurosciences Graduate Program, Stanford University School of Medicine, Stanford, CA 94305, USA
[d] Department of Anesthesiology, University of Toyama, Toyama 930-0194, Japan

ARTICLE INFO

Keywords:
Microglia
TMEM119
Complex regional pain syndrome
Chronic pain
Sex differences

ABSTRACT

Chronic pain is a common and often debilitating problem that affects 100 million Americans. A better understanding of pain's molecular mechanisms is necessary for developing safe and effective therapeutics. Microglial activation has been implicated as a mediator of chronic pain in numerous preclinical studies; unfortunately, translational efforts using known glial modulators have largely failed, perhaps at least in part due to poor specificity of the compounds pursued, or an incomplete understanding of microglial reactivity. In order to achieve a more granular understanding of the role of microglia in chronic pain as a means of optimizing translational efforts, we utilized a clinically-informed mouse model of complex regional pain syndrome (CRPS), and monitored microglial activation throughout pain progression. We discovered that while both males and females exhibit spinal cord microglial activation as evidenced by increases in Iba1, activation is attenuated and delayed in females. We further evaluated the expression of the newly identified microglia-specific marker, TMEM119, and identified two distinct populations in the spinal cord parenchyma after peripheral injury: TMEM119+ microglia and TMEM119- infiltrating myeloid lineage cells, which are comprised of Ly6G + neutrophils and Ly6G- macrophages/monocytes. Neurons are sensitized by inflammatory mediators released in the CNS after injury; however, the cellular source of these cytokines remains somewhat unclear. Using multiplex *in situ* hybridization in combination with immunohistochemistry, we demonstrate that spinal cord TMEM119+ microglia are the cellular source of cytokines IL6 and IL1β after peripheral injury. Taken together, these data have important implications for translational studies: 1) microglia remain a viable analgesic target for males and females, so long as duration after injury is considered; 2) the analgesic properties of microglial modulators are likely at least in part related to their suppression of microglial-released cytokines, and 3) a limited number of neutrophils and macrophages/monocytes infiltrate the spinal cord after peripheral injury but have unknown impact on pain persistence or resolution. Further studies to uncover glial-targeted therapeutic interventions will need to consider sex, timing after injury, and the exact target population of interest to have the specificity necessary for translation.

1. Introduction

In numerous preclinical pain models, peripheral injury results in the release of inflammatory mediators, such as HMGB1, ATP and CSF1, from primary afferent neuron central terminals (Agalave et al., 2014; Guan et al., 2016; Tsuda et al., 2003). Subsequent action in the spinal cord results in documented conversion of spinal cord microglia from a homeostatic, resting state, to an "activated" state with further release of pro-algesic mediators (Jin, Zhuang, Woolf, & Ji, 2003; Tanga, Nutile-McMenemy, & DeLeo, 2005; Tsuda et al., 2003). Agents that reverse

* Corresponding author at: Department of Anesthesiology, Perioperative & Pain Medicine, 300 Pasteur Drive, ED Stone Grant Building, S007, Stanford, CA 94305.
E-mail address: vivianne@stanford.edu (V.L. Tawfik).

https://doi.org/10.1016/j.ynpai.2022.100106
Received 3 March 2022; Received in revised form 30 September 2022; Accepted 10 October 2022
Available online 12 October 2022

microglial activation decrease nociceptive outcomes such as allodynia and thermal hyperalgesia, suggesting an important contribution of activated microglia to persistent pain (Haight, Forman, Cordonnier, James, & Tawfik, 2019; Ji, Berta, & Nedergaard, 2013; Ledeboer et al., 2005; Tawfik, Nutile-McMenemy, Lacroix-Fralish, & Deleo, 2007). Unfortunately, such observations have failed to translate clinically (Curtin et al., 2017), perhaps due to a lack of specificity of purported glial modulators (Moller et al., 2016), oversimplification in our understanding of microglia reactivity (Ransohoff, 2016), incomplete knowledge of sex-specific effects (Sorge et al., 2011; Sorge et al., 2015), or lack of understanding of the time-dependence of microglial contributions to persistent pain (Huck et al., 2021; Kohno et al., 2018).

Microglia are orchestrators of central nervous system (CNS) development with key functions in synaptic pruning, maturation and remodeling that are now also appreciated as direct contributors to a host of CNS diseases (Frost & Schafer, 2016; Schafer et al., 2012). One major challenge in the study of microglia has been the difficulty distinguishing these cells from infiltrating and perivascular macrophages which express similar myeloid lineage markers, including CD11b, Iba1, and Cx3CR1 (Butovsky et al., 2014). Transmembrane protein 119 (TMEM119) was recently identified as a microglia-specific marker in the CNS with stable expression patterns in the brain throughout development in mice and humans (Bennett et al., 2016; Satoh et al., 2016). As such, TMEM119 may provide a unique tool for discerning the exclusive contribution of microglia, and no other myeloid lineage cells, to chronic pain after peripheral injury. This would be particularly important because targeting both microglia and peripheral myeloid cells may hinder injury resolution, especially in the early stages after injury when peripheral macrophages (Loi et al., 2016) and neutrophils (Parisien et al., 2022) are key to tissue healing and protective against the transition to chronic pain.

Limited prior studies have evaluated TMEM119 expression after peripheral injury. Bennett et al. (2016) performed sciatic nerve crush and noted "no loss of TMEM119^{+} microglia" at the dorsal root entry zone at 4 days post-injury. Whether the actual expression level of TMEM119 in the CNS changed after injury is unclear. More recently, TMEM119 levels were found to change in the brain in a model of multiple sclerosis-related chronic neuroinflammation (Grassivaro et al., 2020). Additionally, one study in a preclinical pain model focused on IL-10 gene therapy and found that spinal cord mRNA levels of TMEM119 increase after peripheral nerve injury and this increase was mitigated by intrathecal IL-10 (Vanderwall et al., 2018). While these studies hint at a correlation between TMEM119 expression and microglial activation, it remains unknown if, when, and to what extent TMEM119 expression levels change in the spinal cord after pain-producing peripheral injury and whether such potential changes are sex-specific.

We undertook the present study to evaluate the onset and duration of spinal microglial activation using the microglia-specific marker TMEM119 in male and female mice in the unilateral tibial fracture and casting model of complex regional pain syndrome (CRPS) (Birklein, Ibrahim, Schlereth, & Kingery, 2018). Importantly, we also sought to identify the cellular source of inflammatory cytokines, IL6 and IL1β, released in the CNS that sensitize neurons and contribute to hyperexcitability after injury (Clarkson et al., 2017).

2. Materials and methods

2.1. Animals

All procedures were approved by the Stanford University Administrative Panel on Laboratory Animal Care and the Veterans Affairs Palo Alto Health Care System Institutional Animal Care and Use Committee in accordance with American Veterinary Medical Association guidelines and the International Association for the Study of Pain. Mice (C57BL/6J, Jax #00664, 9–11 weeks upon arrival, 11–12 weeks at study initiation; TMEM119-2A-EGFP (TMEM119-eGFP), Jax #031823, 9–11 weeks upon arrival, 11–12 weeks at study initiation) were housed 2–5 per cage and maintained on a 12-hour light/dark cycle in a temperature-controlled environment with *ad libitum* access to food and water. Male mice weighed approximately 25 g at the start of the study, and female mice weighed approximately 20 g at the start of the study.

2.2. Tibial fracture/casting CRPS model

Mice were anesthetized with isoflurane and underwent a closed right distal tibia fracture followed by casting, as previously described (Tajerian et al., 2015). Briefly, the right hind limb was wrapped in gauze and a hemostat was used to make a closed fracture of the distal tibia. The hind limb was then wrapped in casting tape (ScotchCast™ Plus) from the metatarsals of the hind paw up to a spica formed around the abdomen to ensure that the cast did not slip off. The cast over the paw was applied only to the plantar surface with a window left open over the dorsum of the paw and ankle to prevent constriction when post-fracture edema developed. Mice were inspected throughout the post-operative period of cast immobilization to ensure that the cast was properly positioned. At 3 weeks post-fracture, mice were briefly anesthetized, and casts were removed with cast shears. For behavior, mice were tested starting one day after cast removal, as indicated below.

2.3. Behavioral testing

To ensure rigor in our findings and avoid the contribution of experimenter sex to our behavioral data, experimenters were female or there was a female scientist's lab coat in the room during acclimation and testing (Sorge et al., 2014). *In vivo* behavioral testing was performed in a blinded fashion. All testing was conducted between 7:00 am – 1:00 pm in an isolated, temperature- and light-controlled room. Mice were acclimated for 30–60 min in the testing environment within custom clear plastic cylinders (4″ D) on a raised metal mesh platform (24″ H). Mice were randomized by selection from their home cage and placed randomly in a cylinder on the platform; after testing, mouse identification numbers were recorded on the data sheet. Males and females were tested separately and analyzed separately.

2.3.1. Mechanical nociception assays

To evaluate mechanical reflexive hypersensitivity, we used a logarithmically increasing set of 8 von Frey filaments (Stoelting), ranging in gram force from 0.007 to 6.0 g. These were applied perpendicular to the plantar hindpaw with sufficient force to cause a slight bending of the filament. A positive response was characterized as a rapid withdrawal of the paw away from the stimulus filament within 4 s. Using the up-down statistical method (Chaplan, Bach, Pogrel, Chung, & Yaksh, 1994), the 50 % withdrawal mechanical threshold scores were calculated for each mouse and then averaged across the experimental groups. Mechanical nociception testing was performed at 3, 5, and 7 weeks post-fracture.

2.4. Immunohistochemistry

Mice (12 – 20 weeks) were transcardially perfused with 10 % formalin in PBS. Spinal cords (lumbar cord L1 – L5 segments) were dissected from the mice and cryoprotected in 30 % sucrose in PBS and frozen in O.C.T. (Sakura Finetek, Inc.). Spinal cord sections (40 μm) were prepared using a cryostat (Leica Biosystems) and incubated in blocking solution (5 % normal donkey serum and 0.3 % Triton X-100 in PBS) for 1 h at room temperature followed by incubation with primary antibodies at 4 °C, overnight. The following primary antibodies were used: rabbit anti-Iba1 (FUJIFILM Wako #019-19741, 1:500), goat anti-eGFP (Abcam #ab6673, 1:1000) and rabbit anti-TMEM119 (Abcam #ab209064, 1:1000). After extensive wash with 1 % normal donkey serum and 0.3 % Triton X-100 in PBS, sections were incubated with appropriate secondary antibody conjugated to AlexaFluor (Life Technologies, 1:1000) for 2 h at room temperature followed by a series of

washes in 0.1 M PB. Sections were counterstained with DAPI and mounted on slides using Fluoromount aqueous mounting medium (cat. #F4680, Sigma, USA). Images were collected with a Keyence BZ-X810 fluorescent microscope (Keyence) using the sectioning module to remove non-focused light using the 20x, 40x or 60x objective magnification.

2.5. Quantitative histological analysis

We collected 3–6 dorsal horn images per mouse in upper (L1-L2) and lower (L3-L5) lumbar spinal cord with n = 2–4 mice/sex/time point in order to evaluate the relative cellular expression of Iba1 and TMEM119 in the spinal cord dorsal horn. Each image was taken with identical exposure with 0.4 μm-step z-stacks of 52 slices at 20x objective magnification on the Keyence BZ-X810. For expression levels of Iba1 and TMEM119, images were analyzed using ImageJ/FIJI (Schindelin et al., 2012) by outlining the dorsal horn and setting the threshold to detect only the area of staining and not the background. An identical threshold was then set for all the images and expressed as percent staining Iba1 or TMEM119 positive over the entire area of the dorsal horn. The results were then normalized to controls and final data are shown as % $Iba1^+$/control or % $TMEM119^+$/control. To determine the frequency of individual cell types in the spinal cord, images were analyzed in Adobe Photoshop CS6 by blinded manual counting of individual $Iba1^+$ cells and assigning each cell into one of two groups based on relative expression: $Iba1^+TMEM119^+$ cells or $Iba1^+TMEM119^-$ cells. Controls from each time point were similar therefore controls from 3 weeks are shown.

2.6. Sholl analysis for microglial morphology

Lumbar spinal cord was sectioned on a cryostat at 40 μm and microglia were labeled by immunohistochemistry using the rabbit anti-Iba1 antibody (Wako, #019–19 741, 1:500). Dorsal horn localized microglia were imaged using a Keyence BZ-X800 fluorescent microscope (Keyence) using the sectioning module to remove non-focused light using a 20X objective. Each image was taken at the same exposure using 52 z-stacks at 0.4 μm step size. Images were imported into ImageJ/FIJI and binary images were generated using maximum intensity projections of the microglia. The de-speckle tool was first used to automatically remove non-specific background. The Eraser tool was then used to manually eliminate $Iba1^+$ processes within the frame that were clearly not associated with the microglial cell being analyzed. The paint brush tool was used to connect any $Iba1^+$ processes that were removed from the processing steps but seen in raw IHC images. The Sholl analysis plugin in ImageJ/FIJI with a start radius of 0.5 μm and a step size of 1 μm was used to analyze 20 microglia per section with 2 sections per mouse and 3 mice per timepoint per sex.

2.7. Flow cytometry and fluorescence-activated cell sorting (FACS)

Mice were anesthetized with 120 mg/kg ketamine and 5 mg/kg xylazine and perfused with 15 mL ice-cold Medium A (50 mL 1x HBSS without Ca^{2+} or Mg^{2+} (Gibco, 14185052), 750 μL 1 M HEPES (Gibco, 15630080), 556 μL 45 % glucose (Corning, 25-037-CI)). Spinal cords were placed in 2 mL Medium A + 80 μL DNase I (12,400 units/mL, Sigma, 11284932001) until all samples were dissected. Samples were dounce-homogenized, passed through a 100 μm strainer, washed with 5 mL Medium A, and spun down by centrifugation at 340 *g* for 7 min at 4 °C. Supernatant was suctioned, and pellets were re-suspended in 6 mL 25 % Standard Isotonic Percoll (Percoll: GE Healthcare, 17-5445-02 with 10 % 10x PBS) in Medium A. The suspension underwent centrifugation for 20 min at 950 *g* at 4 °C in order to remove myelin. Supernatant was discarded then washed with 5 mL Medium A and spun down by centrifugation at 340 *g* for 7 min at 4 °C. Cells were re-suspended in FACS buffer (5 mM EDTA in 1 % BSA in 1x PBS). The cell suspension was then spun down at 300 *g* for 5 min at 4 °C. FACS buffer was suctioned off, and cells were re-suspended in FACS buffer. All samples were pre-blocked with 1:100 anti-CD16/CD32 (BD Pharmingen, cat #553142) for 5 min at room temperature. A mixture containing all primary antibodies was then added. The following primary antibodies were used for flow cytometry: e450-conjugated anti-CD3 (eBioscience, cat #48-0031-82), e450-conjugated anti-CD19 (eBioscience, cat #48-0193-82), PE-Cy7-conjugated anti-CD45 (Biolegend, cat #103114), APC-conjugated anti-CD11b (Biolegend, cat #101212), and PE-conjugated anti-Ly6G (Biolegend cat #127607). Dead cells were stained with SYTOX Blue (Life Technologies, cat #S34857). All antibodies were added to the samples at 1:100 along with 1:1000 Sytox Blue and placed on ice for 30 min. Samples were spun down for 5 min at 400 *g* at 4 °C, suctioned and replaced with fresh FACS buffer. The suspension was then spun down for 5 min at 400 *g* at 4 °C, supernatant was suctioned off, cells were re-suspended in FACS buffer and passed through 35 μm filter into polystyrene tubes. Samples were analyzed by flow cytometry in an LSRII (BD Biosciences). Flow cytometry analysis was done using FlowJo v10.7.1. Gating strategy was applied identically to all populations by sex as follows: Forward scatter v. side scatter: area -> Single cells (side scatter: width v. side scatter: height and forward scatter: width v. forward scatter: area) -> live cells, $CD3^-CD19^-CD45^+$ -> myeloid lineage, $CD45^+CD11b^+$ -> microglia, $TMEM119^+$ or infiltrating subpopulations, $TMEM119^-$ -> neutrophils, $Ly6G^+$ and myeloid lineage cells, $Ly6G^-$. Flow cytometry was carried out in uninjured controls and in injured mice at 3 weeks post-fracture.

2.8. RNAscope/immunohistochemistry dual labeling

Fluorescent *in situ* hybridization using the RNAscope Multiplex V2-mM Kit (ACD, #323100) was performed in combination with immunohistochemistry to detect cytokine mRNA (*IL6*, *IL1β*) and protein markers (TMEM119 and Iba1), respectively. Briefly, tissues were isolated and processed as described above for immunohistochemistry (see section 2.4). Spinal cord sections (40 μm) were mounted on glass slides and dried 2hr at room temperature then transferred to −80 °C for storage. On Day 1 of RNAscope, slides were submerged in 10 % formalin and incubated for 20 min at 4 °C. Slides were washed with 1XPBS and dehydrated in EtOH as described in the ACD RNAscope protocol. Sections were incubated for 10 min in RNAscope® Hydrogen Peroxide solution, washed in Millipore water, and incubated in RNAscope® ProteaseIV for 10 min (Mm-IL6 probe, #315891) at room temperature. Probes were hybridized at 40 °C for 2hrs and stored overnight in 5X SSC buffer at room temperature. On Day 2 RNAscope, slides were incubated in Amp1, Amp2, and Amp3 solutions as recommended by the ACD RNAscope protocol and HRP-C1 was used to develop HRP signal followed by incubation with Opal™ 570 reagent (1:1000, Akoya Biosciences) and finally HRP Block. Slides were then washed in 1XPBS and blocked with 10 % Normal Donkey Serum, 0.3 % Triton-X 100 for 1 h at room temperature. Slides were shielded from light and incubated with Rabbit anti-Iba1 (FUJIFILM Wako #019-19741, 1:200) and goat anti-eGFP (Abcam #ab6673, 1:200) in 1 % normal donkey serum and 0.3 % Triton X-100 in 1XPBS at 4 °C overnight. Slides were washed 3X in 1XPBS for 5 min each, incubated with AlexaFluor secondary antibodies (anti-goat-A488 and anti-rabbit-A647), and mounted with Fluoromount G with DAPI (ThermoFisher, #00-4959-52). Images of the spinal cord dorsal horn were captured using a Keyence BZ-X810 fluorescent microscope (Keyence) with a 40X objective. Negative control probes (ACD, #321838) were used to assess background levels of RNAscope signal. In order to quantify cytokine expression in TMEM- and TMEM + cells, we captured 4–6 dorsal horn images per mouse in control (non-fracture) or 3 weeks post-fracture (n = 3 per group per sex). We then quantified the number of $Iba1^+$ TMEM119- or $Iba1^+$ TMEM119+ cells which co-localized with either *IL6* or *IL1β* RNAscope signal. Cells were counted as positive for cytokine signal if the cell had at least one puncta within the cell body or major trunk process. All TMEM119- cells were verified to contain an obvious DAPI-positive nucleus. Total numbers of cells

counted for each condition are shown in Supplemental Table 2.

2.9. Study design & statistical analyses

Cohort sizes were determined based on historical data from our laboratory using a power analysis to provide >80 % power to discover 25 % differences with $p < 0.05$ between groups to require a minimum of 4 animals per group per sex for behavioral outcomes, 3 animals per group per sex for flow cytometry analyses and 2 animals per group per sex for IHC analyses. Mice were randomly assigned to experimental

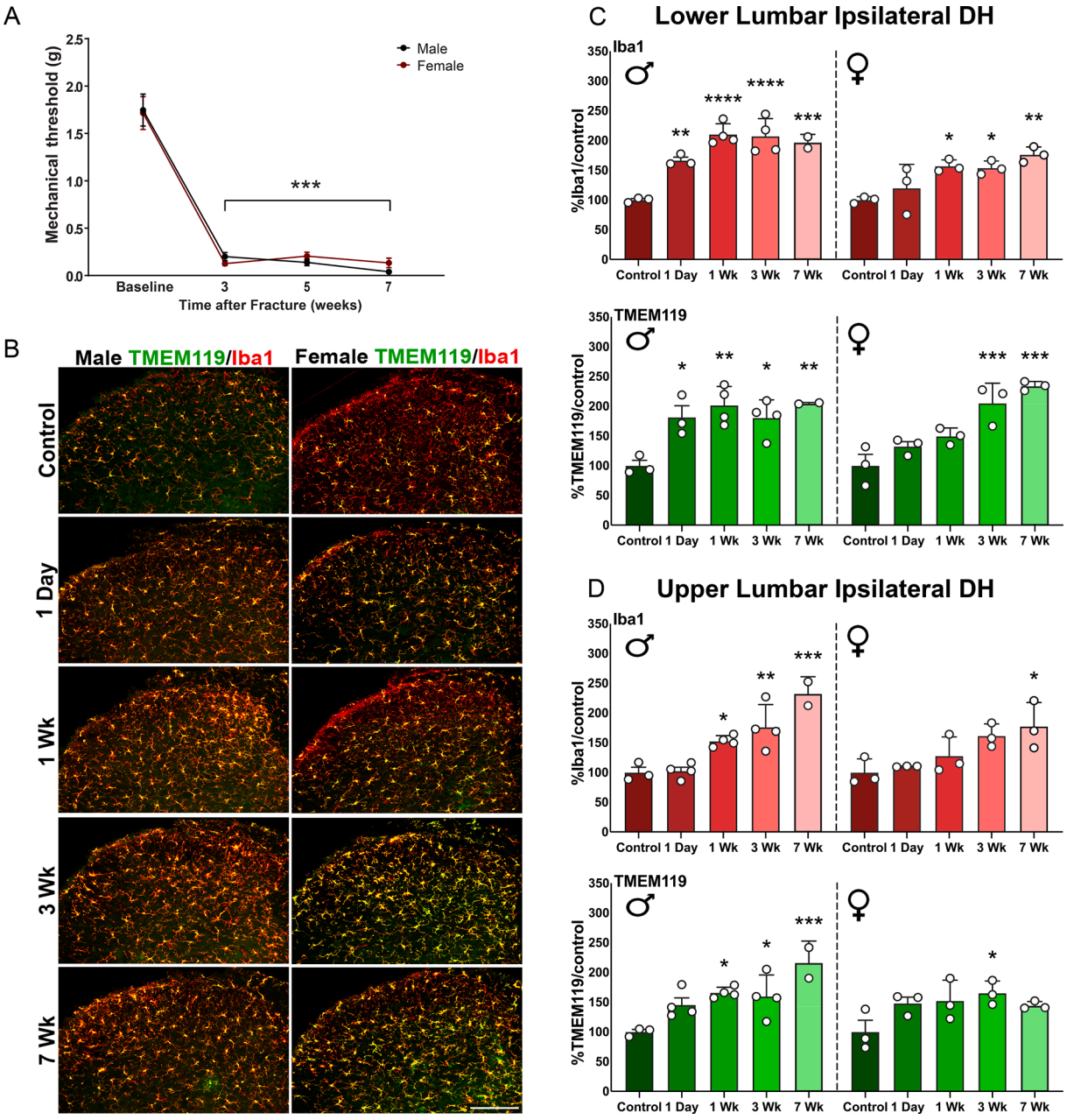

Fig. 1. Tibial fracture/casting results in injured paw allodynia and spinal cord dorsal horn microglial activation in male and female mice. (A) Mechanical allodynia was tested using the von Frey up-down method at multiple time points starting after cast removal at 3 weeks. Both males and females developed profound mechanical sensitivity as indicated by a drop in the mechanical threshold that persisted through 7 weeks post-fracture (n = 5 males, 6 females). Data are presented as mean ± SEM. ***$p < 0.001$ vs sex-matched baseline value by two-way ANOVA with Tukey's multiple comparisons test. (B) Representative immunohistochemistry sections from male and female mice showing lower lumbar spinal cord dorsal horn (DH) labeling of microglia with increasing TMEM119 (green) and Iba1 (red) over time after injury. Images were taken as z-stacks at 20x. Scale bar = 50 um. (C) Densitometry analysis of % Iba1 and % TMEM119 staining in male and female ipsilateral lower lumbar spinal cord DH sections compared to uninjured controls. Significant increases in % Iba1 and % TMEM119 area were noted starting at 1 day and lasting through 7 weeks post-injury in male mice. Female mice had a delayed increase in % Iba1 starting at 1 week and lasting through 7 weeks post-injury while the increase in % TMEM119 was delayed until 3 weeks and lasted through 7 weeks post-injury. (D) Densitometry analysis of % Iba1 and % TMEM119 staining in male and female ipsilateral upper lumbar spinal cord DH sections compared to uninjured controls. Significant increases in % Iba1 and % TMEM119 area were noted starting at 1 week and lasting through 7 weeks post-injury in male mice. Significant increases in % Iba1 were noted at 7 weeks post-injury in female mice with an increase in % TMEM119 only at 3 weeks post-injury. All data are shown by mean + SEM; n = 3–4 per sex per time point, except n = 2 for males at 7 weeks. *$p < 0.05$, **$p < 0.01$, ***$p < 0.001$, ****$p < 0.0001$ vs sex-matched controls by one-way ANOVA with Dunnett's multiple comparisons test. (For interpretation of the references to colour in this figure legend, the reader is referred to the web version of this article.)

groups by cage and behavioral testing performed by a blinded researcher. Researchers remained blinded throughout behavioral, histological and biochemical assessments. Groups were unblinded at the end of each experiment before statistical analysis. Data are expressed as the mean + SEM or +/- SEM with individual data points as indicated in the figure legends. Statistical analysis was performed using GraphPad Prism version 8.4.1 (GraphPad Software). Data were analyzed using paired or unpaired t tests, ordinary-one-way ANOVA followed by Dunnett's or Tukey's multiple comparisons test, or two-way ANOVA with Tukey's post-hoc test, as indicated in the main text or figure captions, as appropriate. The "n" for each individual experiment is listed in the figure legends as well as in Supplemental Table 1.

3. Results

3.1. Tibial fracture/casting results in long-lasting injured paw allodynia

In order to study the TMEM119 expression pattern within the spinal cord and after peripheral injury, we utilized the tibial fracture/casting mouse model of CRPS (Birklein et al., 2018), a form of chronic pain that typically occurs after minor fracture or surgery and immobility/casting. We selected this model because it exhibits a clear acute/peripheral to chronic/central pain transition at 5 weeks post-fracture that is marked by resolution of the peripheral signs of inflammation despite persistent allodynia (Gallagher et al., 2013). We performed right tibial fracture followed by 3 weeks of cast immobilization at which time casts were removed and behavioral testing was performed. Both male and female mice demonstrated significant mechanical allodynia in the ipsilateral hindpaw, as evidenced by a dramatic decrease in the mechanical threshold (Fig. 1A). Significant allodynia was observed through 7 weeks post-fracture, well into the chronic phase of CRPS (Males, $F_{(3,16)} = 83.26$, $p < 0.001$, Females, $F_{(3,20)} = 70$, $p < 0.001$). In previous studies, we have measured allodynia out to 20 weeks post-fracture, at which time gradual improvement to near baseline values was noted (Huck et al., 2021). These results demonstrate that the tibial fracture/casting model produces long-lasting reflexive mechanical allodynia in both male and female mice.

3.2. Spinal cord microglial activation occurs in male and female mice with distinct time courses after peripheral injury

To determine the time course of microglial expression changes in Iba1 and TMEM119 in the CRPS model in male and female mice, spinal cord sections were immunostained with Iba1, a marker of both microglia and infiltrating myeloid lineage cells, and TMEM119, the recently identified microglia-specific marker (Bennett et al., 2016). High background and nonuniform staining hindered our ability to confidently distinguish TMEM119$^+$ cells (microglia) from TMEM119$^-$ cells (infiltrating myeloid lineage cells) in the spinal cord using a commercially available IHC antibody (data not shown). Given the importance of this distinction (TMEM119$^+$ vs TMEM119$^-$) to our current study, we opted to instead use the recently generated knock-in mice expressing EGFP under the TMEM119 promoter (Kaiser & Feng, 2019) for the remaining studies.

In male TMEM119-eGFP mice, increased Iba1 immunoreactivity was observed by 1 day post-fracture in ipsilateral dorsal horn lower lumbar sections, indicating rapid-onset microglial activation in response to injury (Fig. 1B and Supplemental Fig. 1A). While female mice also exhibited clear increases in microglial reactivity (Fig. 1B and Supplemental Fig. 1B), changes in microglial reactivity were attenuated and delayed in females, with an initial increase at 1 week post-fracture. Semi-quantitative analysis of % Iba1$^+$ pixel area showed a significant increase starting at 1 day in males which peaked at 1 week post-fracture and remained elevated through 7 weeks post-fracture. Females showed a significant increase starting at 1 week that was maintained to 7 weeks post-fracture, albeit to a lesser degree at each time point in both lower (Fig. 1C) and upper (Fig. 1D) lumbar ipsilateral dorsal horn.

We next characterized the expression pattern of TMEM119 in the spinal cord at baseline and in the context of painful peripheral injury, as this had not previously been evaluated. In male TMEM119-eGFP mice, overall TMEM119 expression in lower lumbar ipsilateral dorsal horn sections was significantly increased at 1 day and remained elevated through 7 weeks post-fracture, while in females, TMEM119 expression was significantly increased starting at 3 weeks and remained elevated at 7 weeks post-fracture (Fig. 1C). In upper lumbar sections, activation in male TMEM119-eGFP mice was delayed until 1 week post-fracture and remained increased through 7 weeks. Female TMEM119-eGFP mice showed an increased expression that was only significant at 3 weeks post-fracture (Fig. 1D). Collectively, these results suggest a delayed but significant change in microglial activation in upper lumbar spinal regions, consistent with their distance farther from injured afferents, compared to lower lumbar spinal dorsal horn in both male and female mice post-fracture.

3.3. TMEM119 expression distinguishes resident spinal cord microglia from infiltrating Iba1$^+$ cells

When evaluated at high power, all TMEM119$^+$ cells were Iba1$^+$ but not all Iba1$^+$ cells were TMEM119$^+$. Because we saw differences in the overall TMEM119 expression levels between males and females over time after fracture, we next sought to establish the relative frequency of Iba1$^+$TMEM119$^-$ myeloid lineage cells in the spinal cord, as there is evidence for breakdown of the blood-spinal cord barrier in a variety of pain models (Cahill et al., 2014). We created multichannel z-stacks of the spinal cord dorsal horn and evaluated the relative co-expression of Iba1 and TMEM119 in individual cells. With this method, we identified two Iba1$^+$ populations: Iba1$^+$TMEM119$^+$ microglia and Iba1$^+$TMEM119$^-$ myeloid lineage cells (Fig. 2A). In control uninjured male and female mice, there were only trace numbers of Iba1$^+$ TMEM119$^-$ cells (Males, 1.9 ± 0.9, Fig. 2B; Females, 0.9 ± 0.9 Fig. 2C). Tibial fracture/casting resulted in a significant increase in Iba1$^+$TMEM119$^-$ cells in males at 3 weeks (Males, 12.1 ± 1.7, $F_{(4,11)} = 12.88$, $p = 0.0008$) and in females at 7 weeks (Females, 5.8 ± 1.9, $F_{(4,10)} = 3.617$, $p = 0.0243$), suggesting increases in infiltrating myeloid lineage cells. Based on their morphology and parenchymal location in deeper dorsal laminae (Fig. 2A) it is unlikely that these are perivascular macrophages, however, we could not definitely rule this out. In support of the proliferation of Iba1$^+$ TMEM119+ microglia after injury, we found that the absolute number of these cells was significantly increased at 3, and 7 weeks post-fracture in males (Fig. 2D: 3 weeks, 108 ± 4.5, $F_{(4,11)} = 0.2856$, $p = 0.0044$; 7 weeks, 110.2 ± 1.8, $F_{(4,11)} = 0.2856$, $p = 0.0075$), and at 1, 3, and 7 weeks post-fracture in females (Fig. 2E: 1 week, 108.9 ± 4.1, $F_{(4,10)} = 0.5972$, $p = 0.0217$; 3 weeks, 106.6 ± 8.9, $F_{(4,10)} = 0.5972$, $p = 0.0334$; 7 weeks, 125.6 ± 8.3, $F_{(4,10)} = 0.5972$, $p = 0.0011$). We next performed Sholl analysis on TMEM119+ microglia in the spinal cord to better characterize their morphology at 3 weeks post-fracture. As shown in Fig. 3A, control microglia exhibited an extensively ramified morphology compared to the much simpler amoeboid microglia after fracture. In both males (Fig. 3B) and females (Fig. 3C) the complexity of TMEM119$^+$ microglia was significantly decreased post-fracture. Taken together we show both a shift in cellular morphology and an increase in number of both Iba1$^+$ TMEM119$^+$ microglia and Iba1$^+$ TMEM119$^-$ cells in the spinal cord after injury.

3.4. Flow cytometry confirms the existence of distinct infiltrating myeloid lineage populations

To further clarify the cellular identity of Iba1$^+$ TMEM119$^-$ infiltrating cells, we next performed flow cytometry using CD45, CD11b and Ly6G antibodies as well as TMEM119-eGFP. The goal was to more accurately phenotype cells of interest in acutely isolated spinal cord microglia at 3 weeks post-fracture. We identified spinal cord

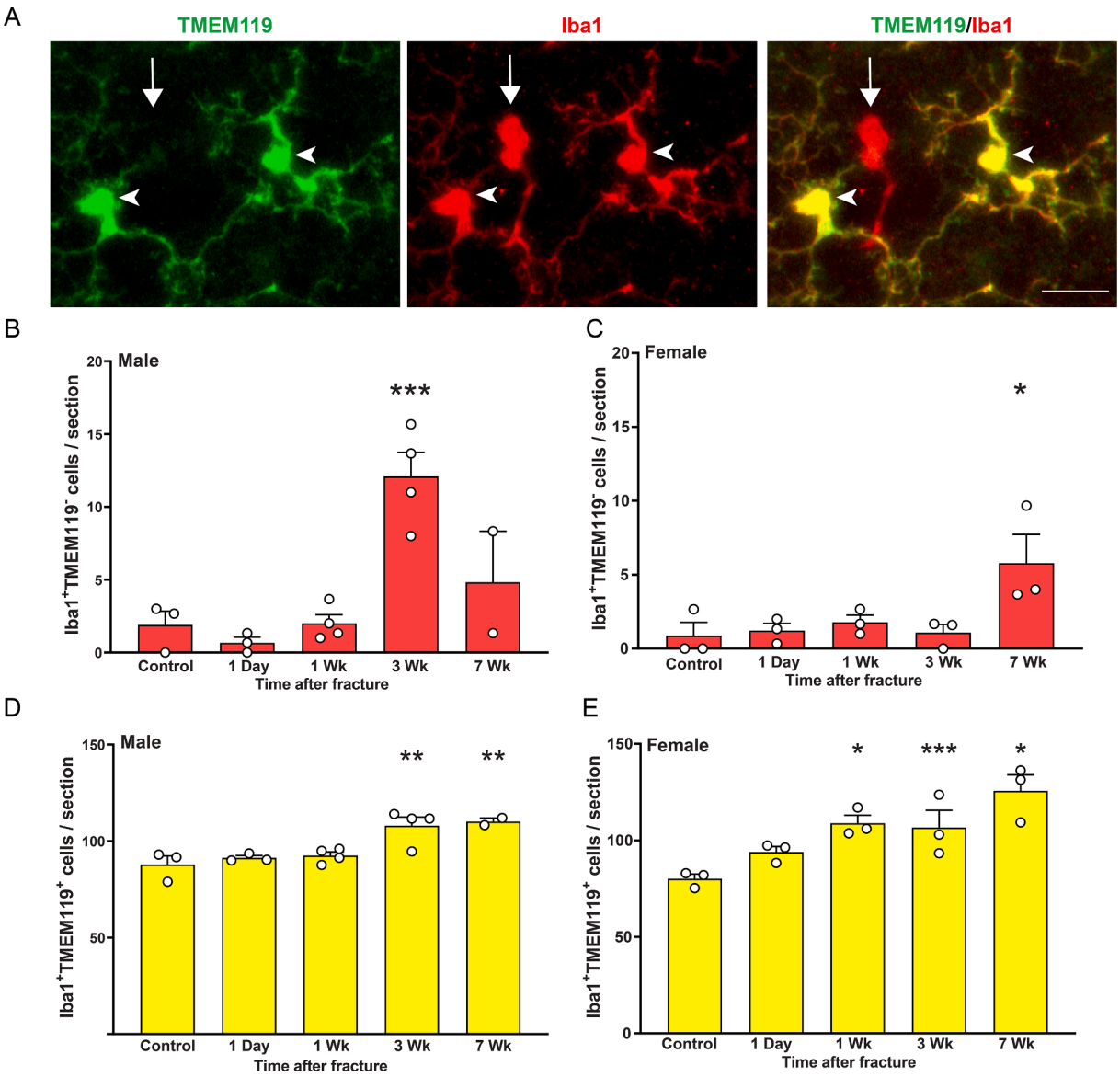

Fig. 2. Relative expression of TMEM119 distinguishes resident microglia from infiltrating myeloid lineage cells in lumbar spinal cord after peripheral injury. (A) Representative immunohistochemistry showing two distinct cell types defined by relative TMEM119 expression: Iba1$^+$ TMEM119$^+$ microglia (arrowhead) and Iba1$^+$ TMEM119$^-$ infiltrating myeloid cell (arrow), with typical amoeboid-like morphology. Scale bar = 15 um. The number of Iba1$^+$ TMEM119$^-$ infiltrating cells and Iba1$^+$ TMEM119$^+$ microglia in the lumbar spinal cord dorsal horn were counted in controls and injured mice at multiple time points after fracture in males (B) and females (C). In controls, Iba1$^+$TMEM119$^-$ cells were rarely seen in either sex, however, an increase in these infiltrating myeloid cells was observed at 3 weeks post-injury in males and at 7 weeks post-injury in females. (D) The number of Iba1$^+$ TMEM119$^+$ microglia increased in males at 3 weeks post-injury and persisted through 7 weeks, while female Iba1$^+$ TMEM119$^+$ microglia increased at 1 week post-injury and persisted through 7 weeks. Data are shown as mean + SEM, 74–178 cells were counted per section, 3–5 spinal cord sections per mouse, n = 2–4 males, n = 3 females per time point. *$p < 0.05$, ***$p < 0.001$ vs sex-matched control by one-way ANOVA with Dunnett's multiple comparisons test.

parenchymal myeloid lineage cells as live CD3$^-$CD19$^-$CD45$^+$CD11b$^+$ cells (Fig. 4A and Supplemental Fig. 2A). Prior to and after fracture in both males (Fig. 4B) and females (Figure C), we observed three populations of myeloid lineage (CD45$^+$CD11b$^+$) cells: TMEM119$^+$ microglia, TMEM119$^-$Ly6G$^+$ neutrophils and TMEM119$^-$Ly6G$^-$ macrophages/monocytes. In controls, the vast majority of CD45$^+$CD11b$^+$ cells were TMEM119$^+$ microglia (Males 96.1 % ± 0.9 % Fig. 4B, Females 96.6 % ± 1.0 % Fig. 4C). At 3 weeks post-fracture, the relative proportion of TMEM119$^+$ microglia decreased to 93.9 % (males, $t_7 = 3.349$, $p = 0.0123$) and 94.4 % (females, $t_5 = 3.175$, $p = 0.0088$) with a reciprocal increase in TMEM119$^-$ cells 5.9 % (males, $t_7 = 3.187$, $p = 0.0153$) and 5.6 % (females, $t_5 = 3.029$, $p = 0.0115$). This TMEM119$^-$ population was further divided into TMEM119$^-$Ly6G$^+$ neutrophils and TMEM119$^-$Ly6G$^-$ macrophages/monocytes which increased in both males (Fig. 4B: myeloid lineage 5.3 %, $t_7 = 2.585$, $p = 0.0362$ and neutrophils 0.6 %, $t_7 = 5.382$, $p = 0.0010$) and females (Fig. 4C: myeloid lineage 4.7 %, $t_5 = 2.216$, $p = 0.0487$ and neutrophils 0.9 %, $t_5 = 2.125p = 0.0571$) after injury. The absolute number of cells was only significantly changed in the case of TMEM119-Ly6G + neutrophils in males after fracture (Supplemental Fig. 3A and B). In addition, TMEM119 median fluorescence intensity (MFI) was not different in males or females after injury (Supplemental Fig. 3C and D) suggesting that proliferation of TMEM119+ microglia, rather than increased expression of TMEM119 was the likely source of the noted increase. In further support of the distinct nature of these infiltrating populations, each exhibited unique size and granularity (seen on forward and side scatter, respectively) and they were clearly discriminated with such gating (Fig. 3A). Taken together, we define the identity of infiltrating

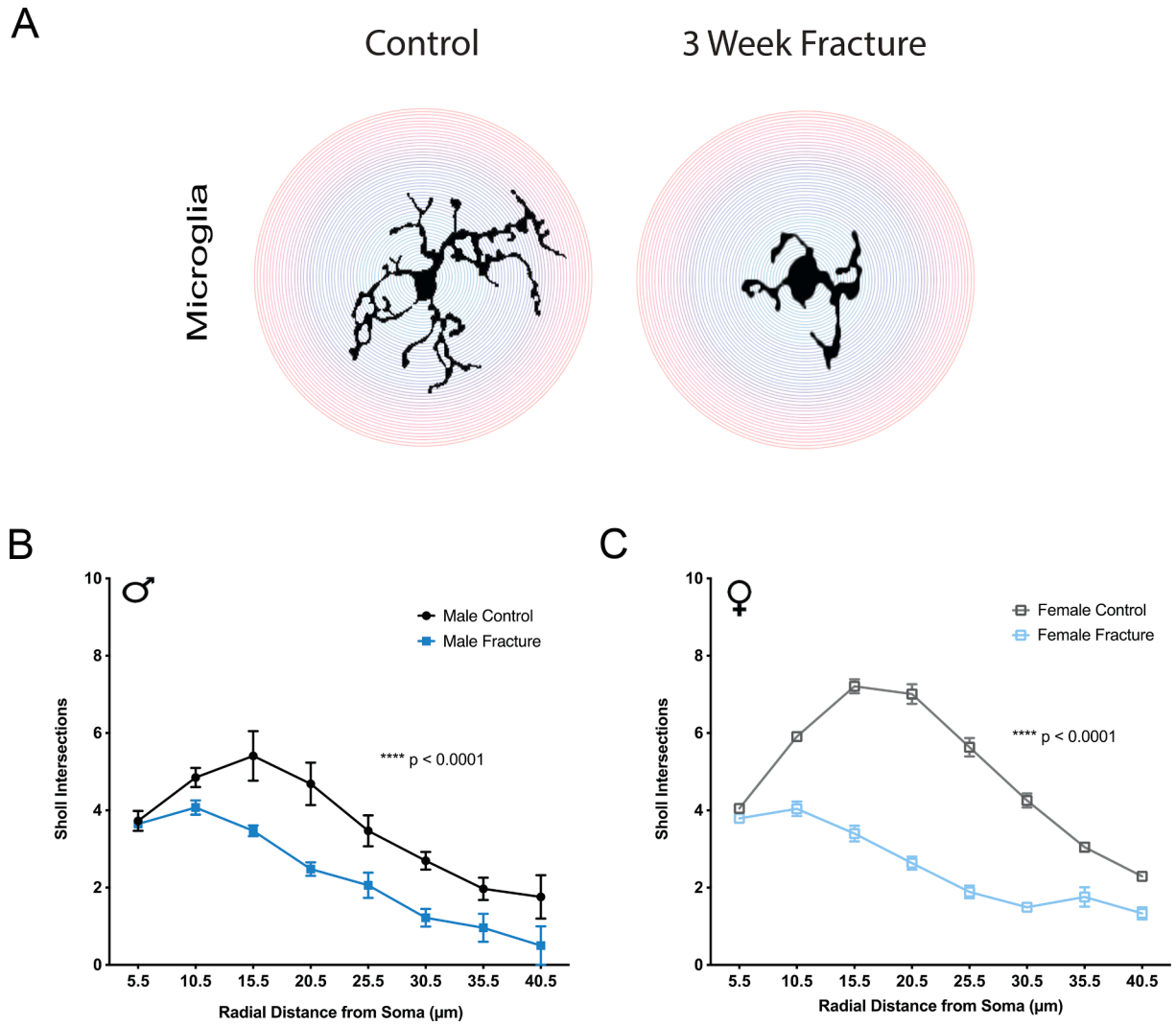

Fig. 3. Sholl Analysis demonstrates de-ramification and shift to an amoeboid morphology in microglia in the lumbar spinal cord of male and female mice after injury. (A) Representative control and post-fracture microglia illustrate a clear shift from ramified to amoeboid morphology after peripheral injury. Concentric circles around the microglia soma used for Sholl analysis spaced at 1 μm apart. Mean distribution plots of the number of Sholl intersections as a function of the distance from the microglial soma for control and 3 weeks post-injury showed a significant decrease in complexity after injury in both males (B) and females (C). Data are shown as mean +/- SEM; n = 3/group, 2 dorsal horn sections per mouse, 20 microglia per section. ****$p < 0.0001$, vs matched subset in controls by two-way ANOVA.

peripheral myeloid lineage cells in the spinal cord after injury in both male and female mice as TMEM119$^-$Ly6G$^+$ neutrophils and TMEM119$^-$Ly6G$^-$ macrophages/monocytes.

3.5. *TMEM119+ microglia are the cellular source of spinal cord cytokines IL6 and IL1β after peripheral injury*

Given the plethora of data in the literature demonstrating increased proinflammatory cytokines (IL6, IL1β) in the spinal cord after peripheral injury (Tawfik, LaCroix-Fralish, Nutile-McMenemy, & DeLeo, 2005) and the effect of such cytokines on neuronal hyperactivity (Clarkson, Kahoud, McCarthy, & Howe, 2017; Goncalves Dos Santos, Delay, Yaksh, & Corr, 2019; Pinho-Ribeiro, Verri, & Chiu, 2017), we next sought to discern which cells (TMEM119+, TMEM119- or others) were the source of these cytokines in this model. To establish whether myeloid lineage cells may express cytokines after injury, we first took advantage of an existing RNA bulk-sequencing dataset in the lab performed on FACS-sorted CD3$^-$CD19$^-$CD45$^+$CD11b$^+$Cx3CR1$^+$ cells in non-injured controls and at 5 weeks post-fracture (dataset generated in Donovan et al., *in preparation*). We found that these cells collectively expressed an increase in IL6 and IL1β mRNA in male (Supp Fig. 4A) but not female (Supp Fig. 4B) mice after injury.

Given the limitations of our existing dataset which included all myeloid cells (TMEM119$^+$ and TMEM119$^-$), we opted to perform dual RNAscope/immunohistochemistry detection to localize the cellular source of cytokines (IL6 and IL1β) in the spinal cord more accurately after peripheral injury. Using this approach, we were able to visualize cytokine mRNA in both male and female lumbar spinal cord at 3 weeks post-fracture using Iba1 and TMEM119 protein to identify the cell types of interest (Fig. 5: IL6, Fig. 6: IL1β). We found a significant increase in the number of Iba1$^+$TMEM119$^+$ cells co-expressing either *IL6* or *IL1β* at 3 weeks post-fracture compared to control non-fracture mice (Supplementary Fig. 5A and B). Further, in post-fracture males, we found that 65 % of Iba1$^+$ TMEM119$^+$ cells co-expressed *IL6* mRNA, while no Iba1$^+$ TMEM119$^-$ cells co-expressed *IL6* mRNA (Fig. 5A). Similarly, in post-fracture females, we found that 68 % of Iba1$^+$ TMEM119+ cells co-expressed *IL6* mRNA, while only 17 % of Iba1$^+$ TMEM119$^-$ cells expressed *IL6* mRNA (Fig. 5B). *IL6* mRNA molecules were found in both the cell bodies as well as processes of Iba1$^+$ TMEM119$^+$ cells. Similarly, we found *IL1β* mRNA localized to Iba1$^+$ TMEM119$^+$ cells (49 % in

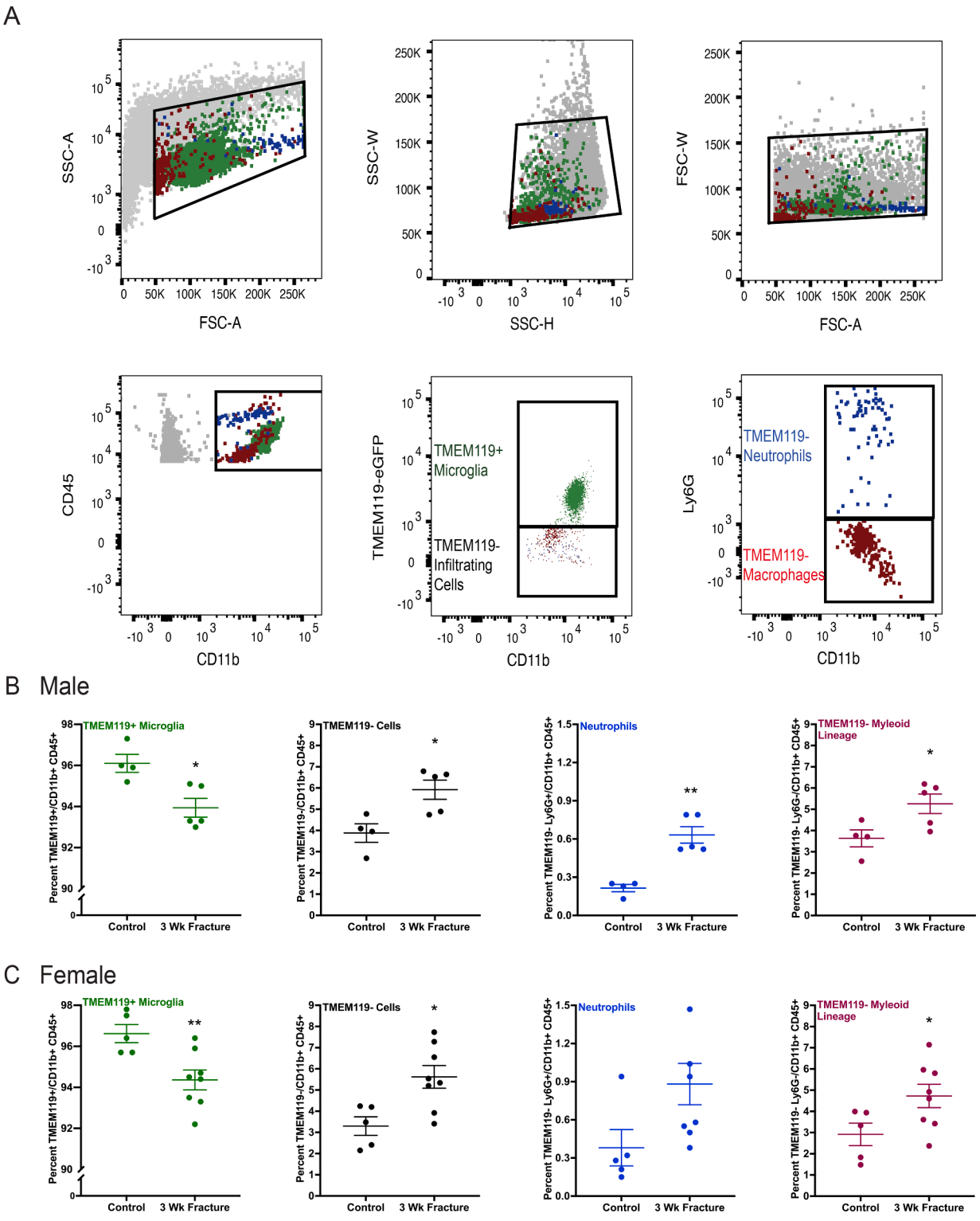

Fig. 4. Flow cytometry analysis confirms the presence of distinct myeloid lineage cells in the lumbar spinal cord of males and females after injury. (A) Representative gating strategy for spinal cord tissue demonstrates two populations of TMEM119$^-$ cells with distinct expression of Ly6G as well as size and granularity as shown by back gating populations. (B) Quantification of male flow cytometry data shows a significant decrease in the relative proportion of TMEM119$^+$ microglia cells and a reciprocal increase in infiltrating TMEM119$^-$ cells at 3 weeks post-injury. This TMEM119$^-$ subset comprises both Ly6G$^+$ neutrophils and Ly6G$^-$ infiltrating myeloid lineage population, both of which are increased at 3 weeks post-injury. (C) Quantification of female flow cytometry data shows a significant decrease in the relative proportion of TMEM119$^+$ microglia cells and a reciprocal increase in infiltrating TMEM119$^-$ cells at 3 weeks post-injury. This TMEM119$^-$ subset comprises both Ly6G$^+$ neutrophils and Ly6G$^-$ infiltrating myeloid lineage populations, however, only the Ly6G$^-$ infiltrating myeloid lineage population was significantly increased at 3 weeks post-injury. Data are shown as individual data points as well as mean +/- SEM; n = 5–8 per time point. *$p < 0.05$, **$p < 0.01$ vs matched subset in controls by unpaired *t*-test.

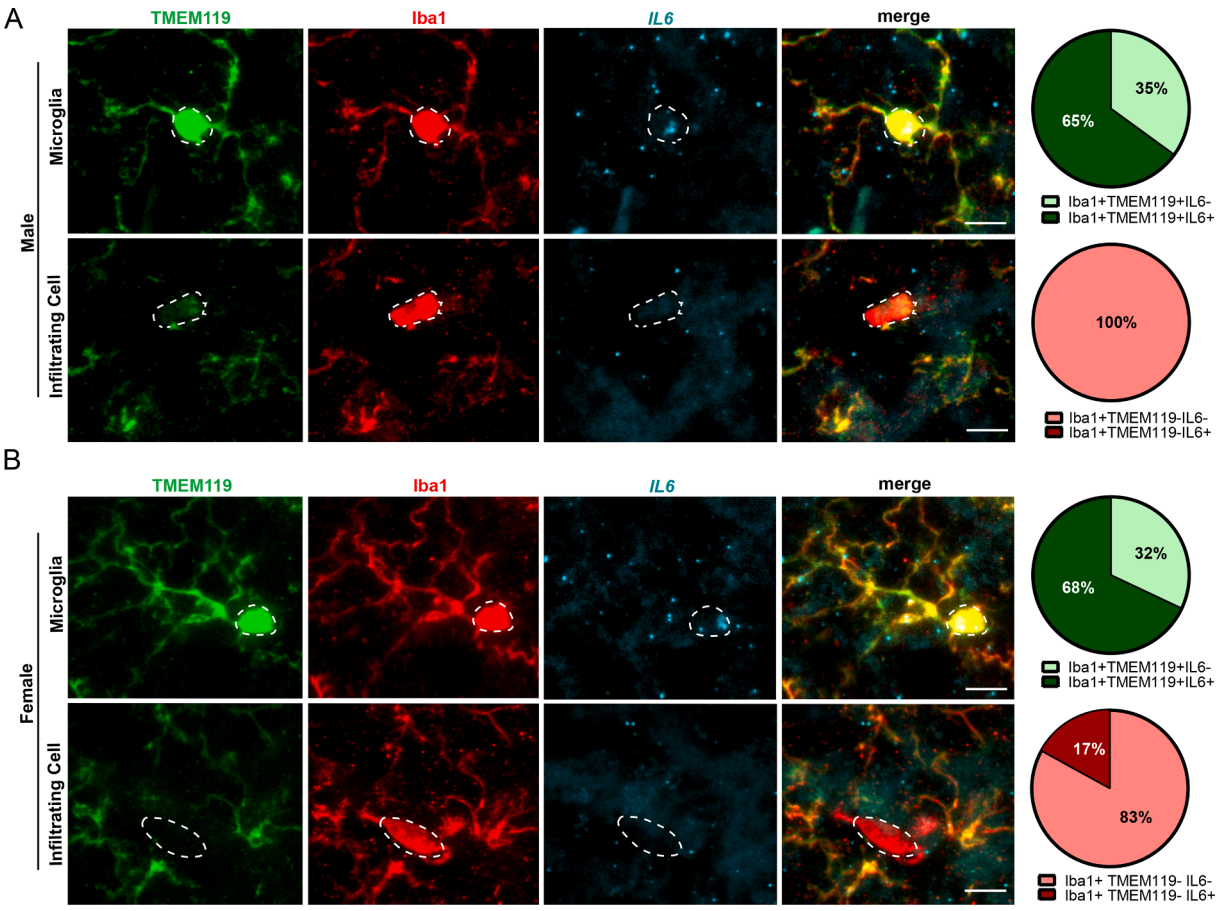

Fig. 5. Cytokine *IL6* mRNA co-localizes with Iba1$^+$ TMEM119$^+$ microglia but not Iba1$^+$ TMEM119$^-$ infiltrating cells at 3 weeks post-fracture. (A) RNAscope performed in combination with immunohistochemistry shows *IL6* mRNA co-localization with Iba1$^+$ TMEM119$^+$ immunoreactive microglia cell bodies and processes (upper panels) but not with rare Iba1$^+$ TMEM119$^-$ infiltrating cells (lower panels) in male mice and (B) female mice 3 weeks post-fracture. Iba1$^+$ TMEM119$^-$ cells display typical amoeboid-like morphology of infiltrating myeloid cells with few-to-no processes (A & B, lower panels). Scale bar = 10 um. Pie charts to the right of image panels display the percentage of total TMEM119+ or TMEM119- microglia that co-colocalized with *IL6* at 3 weeks post fracture.

males, 53 % in females) and not Iba1$^+$ TMEM119$^-$ cells in both males and females (Fig. 6A and B). Of note, at 3 weeks post-fracture (Figs. 5 and 6) a majority of the Iba1$^+$ TMEM119$^-$ cells had an ameboid morphology. These data convincingly demonstrate that Iba1$^+$ TMEM119$^+$ microglia, and not infiltrating myeloid cells, are the primary cellular source of inflammatory cytokines IL6 and IL1β in the spinal cord after peripheral injury.

4. Discussion

The goals of the present study were twofold: 1) to clarify the spinal cord expression of the microglia-specific marker TMEM119; to determine if, when, and to what extent expression levels change after pain-producing peripheral injury, and whether such change is sex-specific, and 2) to establish whether TMEM119$^-$ myeloid cells infiltrate the spinal cord after peripheral injury, and if so, whether they are a cellular source of neuron-sensitizing cytokines. We establish for the first time a sex-specific temporal response of spinal cord TMEM119$^+$ microglia to peripheral injury in our observation that spinal cord microglial activation is attenuated and delayed in females compared to males. Furthermore, we identify distinct populations of TMEM119$^-$ cells in the spinal cord of male and female mice distinguished by Ly6G expression, suggesting that both neutrophils (Ly6G+) and macrophages/monocytes (Ly6G-) infiltrate the spinal cord after peripheral injury, albeit in low numbers. Moreover, we identify TMEM119+ microglia as the cellular source of inflammatory cytokines released in the spinal cord after peripheral injury.

The contribution of microglial activation to chronic pain in preclinical studies remains debated. Some studies have suggested a sex-specific functional contribution of microglia to chronic pain based on improvement in allodynia only in males after microglial-targeted interventions (Fernandez-Zafra et al., 2019; Sorge et al., 2015). While other work has not detected such a sex difference (Agalave et al., 2014; Peng et al., 2016). Our current study suggests that the time course of microglial activation is distinct and delayed in females compared to males, which may account for these discrepant findings. Most studies to date have only evaluated CNS microglia at early time points (days) after injury (Mapplebeck et al., 2018; Mousseau et al., 2018; Sorge et al., 2015). However, we noted Iba1 increases in female spinal cord at 1 week post-fracture with the alteration persisting through at least 7 weeks post-fracture, suggesting that prior studies may have simply missed the timeframe during which these cells are relevant. In agreement, in a model of rheumatoid arthritis, Agalave et al. (2014) found that blocking TLR4-mediated microglial activation by HMGB1 during ongoing inflammation (day 15) or in the post-inflammatory phase (day 48), resulted in decreased hypersensitivity in both male and female mice, with a greater improvement in the latter group. In a follow-up study, Agalave et al. (2021) found that spinal administration of disulfide HMGB1 evoked increased microglia reactivity in male and female mice, but that the mechanism for pain hypersensitivity did not depend on TLR4 in microglia in females. This is consistent with our recent work (Huck et al., 2021), in which we find sexual dimorphism in the involvement of microglial TLR4 in spinal mechanisms of persistent pain. We further identified a role for peripheral TLR4-expressing myeloid cells

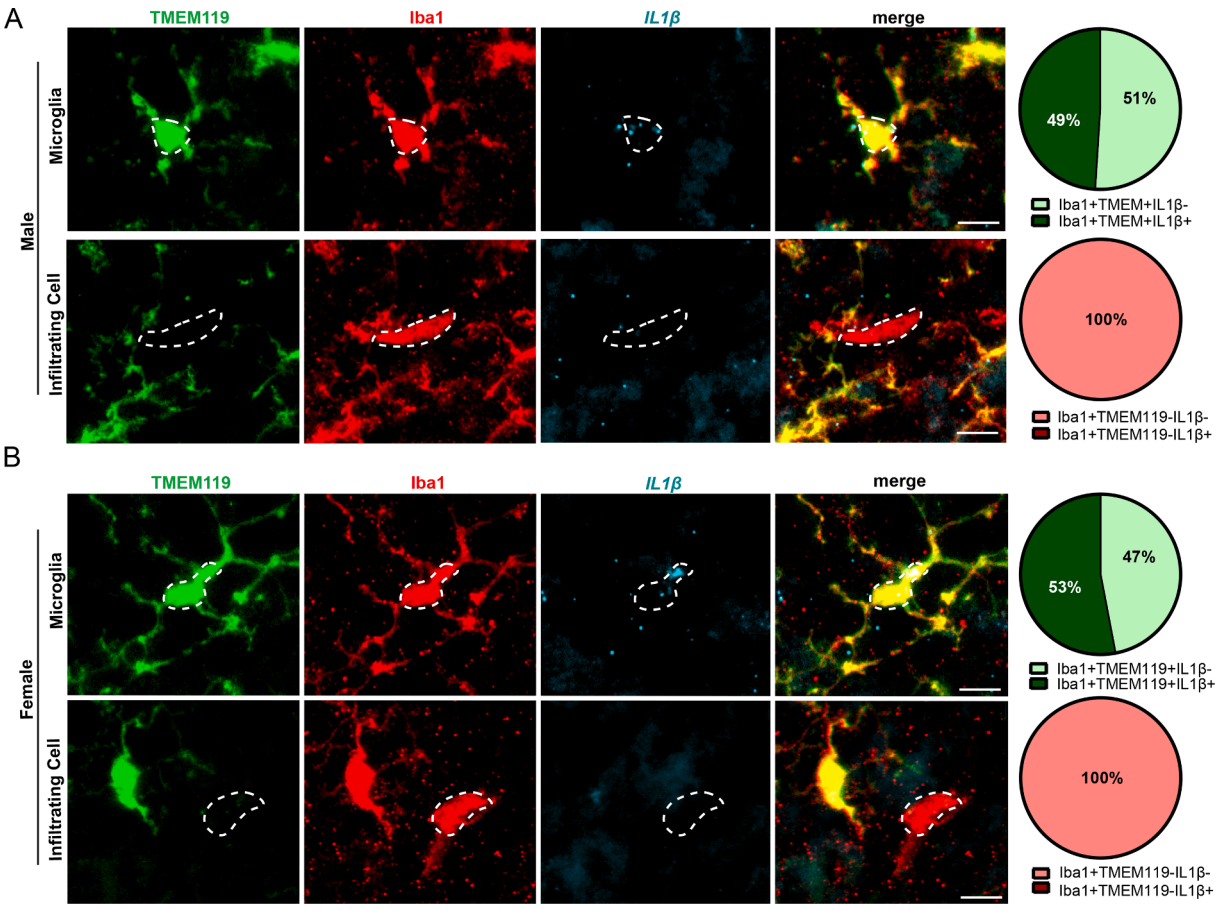

Fig. 6. Cytokine *IL1β* mRNA co-localizes with Iba1$^+$ TMEM119$^+$ microglia but not Iba1$^+$ TMEM119$^-$ infiltrating cells at 3 weeks post-fracture. (A) RNAscope performed in combination with immunohistochemistry shows *IL1β* mRNA co-localization with Iba1$^+$ TMEM119$^+$ immunoreactive microglia cell bodies and processes (upper panels) but not with rare Iba1$^+$ TMEM119- infiltrating cells (lower panels) in male mice and (B) female mice 7 weeks post-fracture. Scale bar = 10 um. Pie charts to the right of image panels display the percentage of total TMEM119+ or TMEM119- microglia that co-colocalized with *IL1β* at 3 weeks post fracture.

or non-TLR4 mediated central microglial mechanisms in female mice. Moreover, we previously demonstrated that microglial modulation may in part contribute to the apparent efficacy of the drug hydroxychloroquine in reducing pain and CRPS-like signs in both female CRPS model mice and women with CRPS (Haight, Johnson, Carroll, & Tawfik, 2020). Finally, new data from our group (Donovan et al. in preparation) demonstrate that microglial depletion in males and females reverses existing allodynia in the tibial fracture/casting model of CRPS. Preclinical model-specific relative contributions of microglia as well as temporal patterns of microglial activation may be additional contributors to divergent outcomes in the efficacy of microglial modulation in males and females. This is consistent with previous work demonstrating variation in microglial activation intensity depending on location of nerve injury from central to peripheral (Colburn, Rickman, & DeLeo, 1999). One clear limitation of our current study is that we did not perform any specific microglia-targeted interventions, and we acknowledge that morphological microglial activation is not necessarily equivalent to microglia-mediated neuroinflammation, as shown in several studies (Corder et al., 2017; Sorge et al., 2015; Ulmann et al., 2008). Regardless, our findings suggest that the timing of glial-targeted interventions may need to be sex-specific, with such interventions being more efficacious in females when initiated in later stages after injury.

In addition to sex-specific timing of microglia activation, we found that immune cell infiltration into the spinal cord dorsal horn also occurs in a delayed fashion in females as evidenced by a peak in Iba1$^+$TMEM119$^-$ cells at 7 weeks (vs 3 weeks in males). Further categorization of this TMEM119$^-$ population based on expression of the neutrophil-specific marker Ly6G revealed the presence of both infiltrating macrophages and neutrophils in the spinal cord of males and females at 3 weeks post-fracture. Previous research suggests that all myeloid cell populations do not contribute equally to inflammatory pain (Ghasemlou, Chiu, Julien, & Woolf, 2015; Tawfik et al., 2020). In plantar incision and CFA models of inflammation, CD11b$^+$Ly6G$^-$ myeloid cells and CD11b$^+$Ly6G$^+$ neutrophils have been found to infiltrate the injury site (Ghasemlou et al., 2015). Depletion of CD11b$^+$Ly6G$^-$ myeloid cells reduced mechanical hypersensitivity following both the plantar incision wound and CFA injection, whereas depletion of CD11b$^+$Ly6G$^+$ neutrophils had no effect on pain behaviors, suggesting that only specific myeloid populations contribute directly to inflammatory pain. However, a recent publication from Parisien et al. (2022) found that neutrophil activation protects against the development of chronic pain. Depletion of neutrophils delayed pain resolution in mice. In contrast, peripheral injection of neutrophils or substances released by neutrophils, S100A8/A9 proteins, prevented the development of long-lasting pain by an anti-inflammatory drug. Interestingly, using the partial sciatic nerve ligation model of neuropathic pain only in male mice, Denk et al. (2016) found small numbers of CD11b$^+$Ly6G$^+$ neutrophils in the spinal cord but almost no infiltrating CD11b$^+$Ly6G$^-$ macrophages by flow cytometry. The difference between that work and the current findings may be related to differences in blood-spinal cord barrier permeability between the injury/pain models employed or the time point evaluated. The tibial fracture/casting model of CRPS likely engages both inflammatory and neuropathic mechanisms, perhaps similar to chemotherapy-induced peripheral neuropathy models in

which the permeability of the blood-spinal cord-barrier is increased and infiltrating monocytes are observed in the spinal cord (Montague-Cardoso et al., 2020). Further work is needed to understand the contributions of infiltrating cells into the spinal cord and their effects on the transition from acute to chronic pain.

Myeloid lineage markers such as Iba1, CD11b, and CX3CR1 are not sufficient to discriminate between microglia and other myeloid lineage cells in the CNS, an issue with critical implications for understanding cell-specific contributions to pathological conditions (Butovsky et al., 2014; Mathys et al., 2017). Highlighting this concept, a new study used single cell RNAseq to demonstrate that a specific population of TMEM119^{-} meningeal macrophages expressing CD163 may actually act in a pro-resolution manner to resolve peripheral injury-induced pain (Niehaus, Taylor-Blake, Loo, Simon, & Zylka, 2021). In our current study, TMEM119- cells are present at earlier time points, but are not significant until 3 weeks post-fracture. This suggests that either it takes time for these cells to enter the parenchyma in large numbers, or that those that enter the parenchyma then proliferate over time.

TMEM119 has been proposed as a microglia-specific marker that can be used to distinguish between such myeloid populations (Bennett et al., 2016; Satoh et al., 2016). TMEM119 is a type IA single-pass transmembrane protein with a role in osteoblast differentiation (Hisa et al., 2011) that is a direct target of Tgfβ1-Smad2 signaling during microglial development (Attaai et al., 2018). It is possible that in our studies, peripheral injury-induced microglial activation triggered the Tgfβ1-Smad2 developmental program to increase TMEM119 levels in existing resident spinal cord microglia in addition to an increase in proliferation of TMEM119^{+} cells. Another possibility is that TMEM119^{-} myeloid cells, which infiltrate the CNS early after injury, may have actually turned on expression of TMEM119 as has been shown in development (Grassivaro et al., 2020). Following microglia depletion in the brain, Ly6C^{hi} monocytes have been observed within the CNS, independent of blood-brain-barrier breakdown, and express several microglia markers including TMEM119 (Lund et al., 2018). Several other recent studies have reported infiltrating macrophages and monocytes taking on microglia-like phenotypes and transcriptomes after injury (Chen et al., 2020; Grassivaro et al., 2020). Chen et al. (2020) found that infiltrating monocytes develop a microglia-like identity characterized by ramified morphology and expression of TMEM119 in the brain following neonatal stroke. Importantly, in an adult ischemic stroke model, Young et al. (2021) observed incongruent TMEM119 protein levels by immunohistochemistry compared to western blot, concluding that TMEM119 could not be reliably used to distinguish between microglia and infiltrating macrophages in all contexts. While infiltrating peripheral cells were identified as TMEM119^{-} in our study, further work using fate mapping such as with CCR2-CreER mice (Chen et al., 2020), are needed to investigate the possibility that some of these cells may take on, or have already taken on, TMEM119 expression in the spinal cord following peripheral injury. In addition, future studies aimed at clarifying the region-specific function of microglia in general, and TMEM119 in particular, are also needed as these cells likely exhibit heterogeneity even within the spinal cord (Grabert et al., 2016; Niehaus et al., 2021). Transcriptome studies focused on understanding sex-specific characteristics of microglia in the spinal cord are starting to identify additional genes or pathways that may further dissect the complex contribution of microglia to male vs female pain (Fernandez-Zafra et al., 2019).

In summary, we characterize the time course of TMEM119^{+} microglial activation in the spinal cord after injury in both males and females and identify a delayed increase in Iba1 and TMEM119 expression in females that persists well into the chronic phase. Finally, we find increases in CD11b^{+}TMEM119^{-} myeloid populations including Ly6G^{+} neutrophils and Ly6G^{-} myeloid lineage in the spinal cord in this mixed neuropathic and inflammatory model. Importantly, these infiltrating cells were small in number and were not found to be the cellular source of cytokines in the spinal cord after peripheral injury, which instead localized to TMEM119^{+} microglia. Further studies to uncover glial-targeted therapeutic interventions will need to consider sex, timing after injury, and exact target population of interest to have the specificity needed for translation.

Declaration of Competing Interest

The authors declare that they have no known competing financial interests or personal relationships that could have appeared to influence the work reported in this paper.

Data availability

Data will be made available on request.

Acknowledgements

This work was supported by National Institutes of Health (NIH) Grant R35GM137906 (V.L.T.), the Rita Allen Foundation Award in Pain (V.L.T.), McCormick-Gabilan Faculty Fellowship (V.L.T.) and funding from the Department of Anesthesiology, Perioperative & Pain Medicine at Stanford University (V.L.T). Research reported in this publication was supported by the National Institute on Drug Abuse of the National Institutes of Health under Award Number T32DA035165 (L.J.D). The content is solely the responsibility of the authors and does not necessarily represent the official views of the National Institutes of Health. G. P.B.M. is supported by a National Defense Science and Engineering Graduate (NDSEG) Fellowship Award. Additional support was provided to Y.T. from the University of Toyama and to H.S. from the University of Soochow. The authors wish to thank Dr. Liana Bonanno for assistance with FACS set-up.

Appendix A. Supplementary data

Supplementary data to this article can be found online at https://doi.org/10.1016/j.ynpai.2022.100106.

References

Agalave, N.M., Larsson, M., Abdelmoaty, S., Su, J., Baharpoor, A., Lundback, P., Svensson, C.I., 2014. Spinal HMGB1 induces TLR4-mediated long-lasting hypersensitivity and glial activation and regulates pain-like behavior in experimental arthritis. Pain 155 (9), 1802–1813. https://doi.org/10.1016/j.pain.2014.06.007.

Agalave, N.M., Rudjito, R., Farinotti, A.B., Khoonsari, P.E., Sandor, K., Nomura, Y., Svensson, C.I., 2021. Sex-dependent role of microglia in disulfide high mobility group box 1 protein-mediated mechanical hypersensitivity. Pain 162 (2), 446–458. https://doi.org/10.1097/j.pain.0000000000002033.

Attaai, A., Neidert, N., von Ehr, A., Potru, P.S., Zoller, T., Spittau, B., 2018. Postnatal maturation of microglia is associated with alternative activation and activated TGFbeta signaling. [182]. Glia 66 (8), 1695–1708. https://doi.org/10.1002/glia.23332.

Bennett, M.L., Bennett, F.C., Liddelow, S.A., Ajami, B., Zamanian, J.L., Fernhoff, N.B., Barres, B.A., 2016. New tools for studying microglia in the mouse and human CNS. [164]. E1746 Proc Natl Acad Sci U S A 113 (12), E1738. https://doi.org/10.1073/pnas.1525528113.

Birklein, F., Ibrahim, A., Schlereth, T., Kingery, W.S., 2018. The Rodent Tibia Fracture Model: A Critical Review and Comparison With the Complex Regional Pain Syndrome Literature. J Pain 19 (10), 1102.e1101–1102.e1119. https://doi.org/10.1016/j.jpain.2018.03.018.

Butovsky, O., Jedrychowski, M.P., Moore, C.S., Cialic, R., Lanser, A.J., Gabriely, G., Weiner, H.L., 2014. Identification of a unique TGF-beta-dependent molecular and functional signature in microglia. [190]. Nat Neurosci 17 (1), 131–143. https://doi.org/10.1038/nn.3599.

Cahill, L.S., Laliberte, C.L., Liu, X.J., Bishop, J., Nieman, B.J., Mogil, J.S., Henkelman, R. M., 2014. Quantifying blood-spinal cord barrier permeability after peripheral nerve injury in the living mouse. Mol Pain 10, 60. https://doi.org/10.1186/1744-8069-10-60.

Chaplan, S.R., Bach, F.W., Pogrel, J.W., Chung, J.M., Yaksh, T.L., 1994. Quantitative assessment of tactile allodynia in the rat paw. J Neurosci Methods 53 (1), 55–63. https://doi.org/10.1016/0165-0270(94)90144-9.

Chen, H.R., Sun, Y.Y., Chen, C.W., Kuo, Y.M., Kuan, I.S., Tiger Li, Z.R., Kuan, C.Y., 2020. Fate mapping via CCR2-CreER mice reveals monocyte-to-microglia transition in development and neonatal stroke. Sci Adv 6 (35), eabb2119. https://doi.org/10.1126/sciadv.abb2119.

Clarkson, B.D.S., Kahoud, R.J., McCarthy, C.B., Howe, C.L., 2017. Inflammatory cytokine-induced changes in neural network activity measured by waveform analysis of high-content calcium imaging in murine cortical neurons. Sci Rep 7 (1), 9037. https://doi.org/10.1038/s41598-017-09182-5.

Colburn, R.W., Rickman, A.J., DeLeo, J.A., 1999. The effect of site and type of nerve injury on spinal glial activation and neuropathic pain behavior. Exp Neurol 157 (2), 289–304. https://doi.org/10.1006/exnr.1999.7065.

Corder, G., Tawfik, V.L., Wang, D., Sypek, E.I., Low, S.A., Dickinson, J.R., Scherrer, G., 2017. Loss of mu opioid receptor signaling in nociceptors, but not microglia, abrogates morphine tolerance without disrupting analgesia. [106]. Nat Med 23 (2), 164–173. https://doi.org/10.1038/nm.4262.

Curtin, C.M., Kenney, D., Suarez, P., Hentz, V.R., Hernandez-Boussard, T., Mackey, S., Carroll, I.R., 2017. A Double-Blind Placebo Randomized Controlled Trial of Minocycline to Reduce Pain After Carpal Tunnel and Trigger Finger Release. J Hand Surg Am 42 (3), 166–174. https://doi.org/10.1016/j.jhsa.2016.12.011.

Denk, F., Crow, M., Didangelos, A., Lopes, D.M., McMahon, S.B., 2016. Persistent Alterations in Microglial Enhancers in a Model of Chronic Pain. [551]. *Cell Rep* 15 (8), 1771–1781. https://doi.org/10.1016/j.celrep.2016.04.063.

Fernandez-Zafra, T., Gao, T., Jurczak, A., Sandor, K., Hore, Z., Agalave, N.M., Svensson, C.I., 2019. Exploring the transcriptome of resident spinal microglia after collagen antibody-induced arthritis. [191]. Pain 160 (1), 224–236. https://doi.org/10.1097/j.pain.0000000000001394.

Frost, J.L., Schafer, D.P., 2016. Microglia: Architects of the Developing Nervous System. Trends Cell Biol 26 (8), 587–597. https://doi.org/10.1016/j.tcb.2016.02.006.

Gallagher, J.J., Tajerian, M., Guo, T., Shi, X., Li, W., Zheng, M., Clark, J.D., 2013. Acute and chronic phases of complex regional pain syndrome in mice are accompanied by distinct transcriptional changes in the spinal cord. [518]. Mol Pain 9, 40. https://doi.org/10.1186/1744-8069-9-40.

Ghasemlou, N., Chiu, I. M., Julien, J. P., & Woolf, C. J. (2015). CD11b+Ly6G- myeloid cells mediate mechanical inflammatory pain hypersensitivity. *Proc Natl Acad Sci U S A, 112*(49), E6808-6817. doi:10.1073/pnas.1501372112.

Goncalves Dos Santos, G., Delay, L., Yaksh, T.L., Corr, M., 2019. Neuraxial Cytokines in Pain States. Front Immunol 10, 3061. https://doi.org/10.3389/fimmu.2019.03061.

Grabert, K., Michoel, T., Karavolos, M.H., Clohisey, S., Baillie, J.K., Stevens, M.P., McColl, B.W., 2016. Microglial brain region-dependent diversity and selective regional sensitivities to aging. [154]. Nat Neurosci 19 (3), 504–516. https://doi.org/10.1038/nn.4222.

Grassivaro, F., Menon, R., Acquaviva, M., Ottoboni, L., Ruffini, F., Bergamaschi, A., Martino, G., 2020. Convergence between Microglia and Peripheral Macrophages Phenotype during Development and Neuroinflammation. J Neurosci 40 (4), 784–795. https://doi.org/10.1523/JNEUROSCI.1523-19.2019.

Guan, Z., Kuhn, J.A., Wang, X., Colquitt, B., Solorzano, C., Vaman, S., Basbaum, A.I., 2016. Injured sensory neuron-derived CSF1 induces microglial proliferation and DAP12-dependent pain. [158AB]. Nat Neurosci 19 (1), 94–101. https://doi.org/10.1038/nn.4189.

Haight, E.S., Forman, T.E., Cordonnier, S.A., James, M.L., Tawfik, V.L., 2019. Microglial Modulation as a Target for Chronic Pain: From the Bench to the Bedside and Back. Anesth Analg 128 (4), 737–746. https://doi.org/10.1213/ANE.0000000000004033.

Haight, E.S., Johnson, E.M., Carroll, I.R., Tawfik, V.L., 2020. Of mice, microglia, and (wo)men: a case series and mechanistic investigation of hydroxychloroquine for complex regional pain syndrome. Pain Rep 5 (5), e841.

Hisa, I., Inoue, Y., Hendy, G.N., Canaff, L., Kitazawa, R., Kitazawa, S., Kaji, H., 2011. Parathyroid hormone-responsive Smad3-related factor, Tmem119, promotes osteoblast differentiation and interacts with the bone morphogenetic protein-Runx2 pathway. J Biol Chem 286 (11), 9787–9796. https://doi.org/10.1074/jbc.M110.179127.

Huck, N.A., Siliezar-Doyle, J., Haight, E.S., Ishida, R., Forman, T.E., Wu, S., Tawfik, V.L., 2021. Temporal Contribution of Myeloid-Lineage TLR4 to the Transition to Chronic Pain: A Focus on Sex Differences. J Neurosci 41 (19), 4349–4365. https://doi.org/10.1523/JNEUROSCI.1940-20.2021.

Ji, R.R., Berta, T., Nedergaard, M., 2013. Glia and pain: is chronic pain a gliopathy? [27]. Pain 154 (Suppl 1), S10–S28. https://doi.org/10.1016/j.pain.2013.06.022.

Jin, S.X., Zhuang, Z.Y., Woolf, C.J., Ji, R.R., 2003. p38 mitogen-activated protein kinase is activated after a spinal nerve ligation in spinal cord microglia and dorsal root ganglion neurons and contributes to the generation of neuropathic pain. Retrieved from J Neurosci 23 (10), 4017–4022. https://www.ncbi.nlm.nih.gov/pubmed/12764087.

Kaiser, T., Feng, G., 2019. Tmem119-EGFP and Tmem119-CreERT2 Transgenic Mice for Labeling and Manipulating Microglia. [184]. *eneuro* 6 (4). https://doi.org/10.1523/ENEURO.0448-18.2019.

Kohno, K., Kitano, J., Kohro, Y., Tozaki-Saitoh, H., Inoue, K., Tsuda, M., 2018. Temporal Kinetics of Microgliosis in the Spinal Dorsal Horn after Peripheral Nerve Injury in Rodents. [153]. Biol Pharm Bull 41 (7), 1096–1102. https://doi.org/10.1248/bpb.b18-00278.

Ledeboer, A., Sloane, E.M., Milligan, E.D., Frank, M.G., Mahony, J.H., Maier, S.F., Watkins, L.R., 2005. Minocycline attenuates mechanical allodynia and proinflammatory cytokine expression in rat models of pain facilitation. Pain 115 (1–2), 71–83. https://doi.org/10.1016/j.pain.2005.02.009.

Loi, F., Cordova, L.A., Pajarinen, J., Lin, T.H., Yao, Z., Goodman, S.B., 2016. Inflammation, fracture and bone repair. [47]. Bone 86, 119–130. https://doi.org/10.1016/j.bone.2016.02.020.

Lund, H., Pieber, M., Parsa, R., Han, J., Grommisch, D., Ewing, E., Harris, R.A., 2018. Competitive repopulation of an empty microglial niche yields functionally distinct subsets of microglia-like cells. [181]. *Nat Commun* 9 (1), 4845. https://doi.org/10.1038/s41467-018-07295-7.

Mapplebeck, J.C.S., Dalgarno, R., Tu, Y., Moriarty, O., Beggs, S., Kwok, C.H.T., Salter, M. W., 2018. Microglial P2X4R-evoked pain hypersensitivity is sexually dimorphic in rats. [143]. Pain 159 (9), 1752–1763. https://doi.org/10.1097/j.pain.0000000000001265.

Mathys, H., Adaikkan, C., Gao, F., Young, J.Z., Manet, E., Hemberg, M., Tsai, L.H., 2017. Temporal Tracking of Microglia Activation in Neurodegeneration at Single-Cell Resolution. [142]. *Cell Rep* 21 (2), 366–380. https://doi.org/10.1016/j.celrep.2017.09.039.

Moller, T., Bard, F., Bhattacharya, A., Biber, K., Campbell, B., Dale, E., Boddeke, H.W., 2016. Critical data-based re-evaluation of minocycline as a putative specific microglia inhibitor. [26]. Glia 64 (10), 1788–1794. https://doi.org/10.1002/glia.23007.

Montague-Cardoso, K., Pitcher, T., Chisolm, K., Salera, G., Lindstrom, E., Hewitt, E., Malcangio, M., 2020. Changes in vascular permeability in the spinal cord contribute to chemotherapy-induced neuropathic pain. Brain Behav Immun 83, 248–259. https://doi.org/10.1016/j.bbi.2019.10.018.

Mousseau, M., Burma, N.E., Lee, K.Y., Leduc-Pessah, H., Kwok, C.H.T., Reid, A.R., Trang, T., 2018. Microglial pannexin-1 channel activation is a spinal determinant of joint pain. [145]. *Sci Adv* 4 (8), eaas9846. https://doi.org/10.1126/sciadv.aas9846.

Niehaus, J.K., Taylor-Blake, B., Loo, L., Simon, J.M., Zylka, M.J., 2021. Spinal macrophages resolve nociceptive hypersensitivity after peripheral injury. Neuron 109 (8), 1274–1282.e1276. https://doi.org/10.1016/j.neuron.2021.02.018.

Parisien, M., Lima, L.V., Dagostino, C., El-Hachem, N., Drury, G.L., Grant, A.V., Diatchenko, L., 2022. Acute inflammatory response via neutrophil activation protects against the development of chronic pain. Sci Transl Med 14 (644), eabj9954. https://doi.org/10.1126/scitranslmed.abj9954.

Peng, J., Gu, N., Zhou, L., U, B. E., Murugan, M., Gan, W. B., & Wu, L. J, 2016. Microglia and monocytes synergistically promote the transition from acute to chronic pain after nerve injury. [161AB]. *Nat Commun* 7, 12029. https://doi.org/10.1038/ncomms12029.

Pinho-Ribeiro, F.A., Verri Jr., W.A., Chiu, I.M., 2017. Nociceptor Sensory Neuron-Immune Interactions in Pain and Inflammation. Trends Immunol 38 (1), 5–19. https://doi.org/10.1016/j.it.2016.10.001.

Ransohoff, R.M., 2016. A polarizing question: do M1 and M2 microglia exist? [25]. Nat Neurosci 19 (8), 987–991. https://doi.org/10.1038/nn.4338.

Satoh, J., Kino, Y., Asahina, N., Takitani, M., Miyoshi, J., Ishida, T., Saito, Y., 2016. TMEM119 marks a subset of microglia in the human brain. Neuropathology 36 (1), 39–49. https://doi.org/10.1111/neup.12235.

Schafer, D.P., Lehrman, E.K., Kautzman, A.G., Koyama, R., Mardinly, A.R., Yamasaki, R., Stevens, B., 2012. Microglia sculpt postnatal neural circuits in an activity and complement-dependent manner. Neuron 74 (4), 691–705. https://doi.org/10.1016/j.neuron.2012.03.026.

Schindelin, J., Arganda-Carreras, I., Frise, E., Kaynig, V., Longair, M., Pietzsch, T., Cardona, A., 2012. Fiji: an open-source platform for biological-image analysis. Nat Methods 9 (7), 676–682. https://doi.org/10.1038/nmeth.2019.

Sorge, R.E., LaCroix-Fralish, M.L., Tuttle, A.H., Sotocinal, S.G., Austin, J.S., Ritchie, J., Mogil, J.S., 2011. Spinal cord Toll-like receptor 4 mediates inflammatory and neuropathic hypersensitivity in male but not female mice. [183]. J Neurosci 31 (43), 15450–15454. https://doi.org/10.1523/JNEUROSCI.3859-11.2011.

Sorge, R.E., Martin, L.J., Isbester, K.A., Sotocinal, S.G., Rosen, S., Tuttle, A.H., Mogil, J. S., 2014. Olfactory exposure to males, including men, causes stress and related analgesia in rodents. Nat Methods 11 (6), 629–632. https://doi.org/10.1038/nmeth.2935.

Sorge, R.E., Mapplebeck, J.C., Rosen, S., Beggs, S., Taves, S., Alexander, J.K., Mogil, J.S., 2015. Different immune cells mediate mechanical pain hypersensitivity in male and female mice. [155]. Nat Neurosci 18 (8), 1081–1083. https://doi.org/10.1038/nn.4053.

Tajerian, M., Sahbaie, P., Sun, Y., Leu, D., Yang, H.Y., Li, W., David Clark, J., 2015. Sex differences in a Murine Model of Complex Regional Pain Syndrome. Neurobiol Learn Mem 123, 100–109. https://doi.org/10.1016/j.nlm.2015.06.004.

Tanga, F.Y., Nutile-McMenemy, N., DeLeo, J.A., 2005. The CNS role of Toll-like receptor 4 in innate neuroimmunity and painful neuropathy. Proc Natl Acad Sci U S A 102 (16), 5856–5861. https://doi.org/10.1073/pnas.0501634102.

Tawfik, V.L., LaCroix-Fralish, M.L., Nutile-McMenemy, N., DeLeo, J.A., 2005. Transcriptional and translational regulation of glial activation by morphine in a rodent model of neuropathic pain. J Pharmacol Exp Ther 313 (3), 1239–1247. https://doi.org/10.1124/jpet.104.082420.

Tawfik, V.L., Nutile-McMenemy, N., Lacroix-Fralish, M.L., Deleo, J.A., 2007. Efficacy of propentofylline, a glial modulating agent, on existing mechanical allodynia following peripheral nerve injury. Brain Behav Immun 21 (2), 238–246. https://doi.org/10.1016/j.bbi.2006.07.001.

Tawfik, V.L., Huck, N.A., Baca, Q.J., Ganio, E.A., Haight, E.S., Culos, A., Gaudilliere, B., 2020. Systematic Immunophenotyping Reveals Sex-Specific Responses After Painful Injury in Mice. Front Immunol 11 (1652), 1652. https://doi.org/10.3389/fimmu.2020.01652.

Tsuda, M., Shigemoto-Mogami, Y., Koizumi, S., Mizokoshi, A., Kohsaka, S., Salter, M.W., Inoue, K., 2003. P2X4 receptors induced in spinal microglia gate tactile allodynia after nerve injury. Nature 424 (6950), 778–783. https://doi.org/10.1038/nature01786.

Ulmann, L., Hatcher, J.P., Hughes, J.P., Chaumont, S., Green, P.J., Conquet, F., Rassendren, F., 2008. Up-regulation of P2X4 receptors in spinal microglia after

peripheral nerve injury mediates BDNF release and neuropathic pain. J Neurosci 28 (44), 11263–11268. https://doi.org/10.1523/JNEUROSCI.2308-08.2008.

Vanderwall, A.G., Noor, S., Sun, M.S., Sanchez, J.E., Yang, X.O., Jantzie, L.L., Milligan, E. D., 2018. Effects of spinal non-viral interleukin-10 gene therapy formulated with d-mannose in neuropathic interleukin-10 deficient mice: Behavioral characterization, mRNA and protein analysis in pain relevant tissues. Brain Behav Immun 69, 91–112. https://doi.org/10.1016/j.bbi.2017.11.004.

Young, K.F., Gardner, R., Sariana, V., Whitman, S.A., Bartlett, M.J., Falk, T., Morrison, H. W., 2021. Can quantifying morphology and TMEM119 expression distinguish between microglia and infiltrating macrophages after ischemic stroke and reperfusion in male and female mice? J Neuroinflammation 18 (1), 58. https://doi.org/10.1186/s12974-021-02105-2.